2017 13th International Conference on Computational Intelligence and Security

Salient Object Detection via Nonconvex Structured Matrix Decomposition

Xiaoting Zhang
College of Mathematics and Statistics
Shenzhen University
Shenzhen, China
Email: 1229218718@qq.com

Xiaoli Sun*
College of Mathematics and Statistics
Shenzhen University
Shenzhen, China
Email: xlsun@szu.edu.cn

Xiujun Zhang
School of Electronic and Communication Engineering
Shenzhen Polytechnic
Shenzhen, China
Email: zhangxiujun@szpt.edu.cn

***Abstract*—In the salient object detection, the feature matrix of an image can be represented as a low-rank matrix plus a sparse matrix, corresponding to the background and the salient regions, respectively. Generally, the rank function is approximated by the nuclear norm. However, solving the nuclear norm minimization problem usually leads to a suboptimal solution. To address this problem, we propose a novel nonconvex structure matrix decomposition model, where using a nonconvex surrogate ($i.e.$, the l_1 norm of logistic function) on the singular values of a matrix to approximate the rank function. In addition, our model contains two structural regularizations: a group sparsity induced norm regularization to explore the relationship between each superpixel, making salient object highlighted consistently, and a Laplacian regularization to increase the distance between salient regions and non-salient regions in feature space. Finally, high-level priors are integrated to our model. Experimental results show that our model can achieve better performance compared with the state-of-the-art methods.**

***Keywords*-salient object detection; nonconvex; low rank; matrix decomposition; group sparsity**

I. Introduction

Saliency detection aims to detect the attractive objects on images, which is similar to the selective mechanism of human vision [5]. In recent years, more and more research efforts have been conducted for visual saliency analysis. Rather than eye fixation prediction [6] just predicting a few salient points in an image, salient object detection aims to select outstanding and interesting regions from the complex scenes. As an essential pre-processing step, this technique is widely applied to various computer vision fields, including image segmentation [7], compression [8] and object discovery [9], etc. Generally speaking, saliency algorithms can be classified into two major categories ($i.e.$ bottom-up and top-down schemes [10], [11]) depending on whether the prior knowledge is used or not. And high-level priors are integrated in our model to promote the performance.

In our model, we treat the salient object detection as a problem of low-rank and structured-sparse matrix decomposition. In the traditional representation-based low rank matrix approximation problem, the nuclear norm is generally used as a convex surrogate of the rank function. However, the nuclear norm is a loose approximation of the rank function and usually leads to a suboptimal solution. Therefore, many nonconvex regularizers have been proposed to address this problem. In [12], Lu et al. proposed to use a family of nonconvex surrogates of l_0 norm on the singular values to approximate the rank function and its nonconvex nonsmooth minimization problem was solved by an iteratively reweighted nuclear norm algorithm. Motivated by its related theory, the reference [15] sought the scale parameter iteratively by using full MAP (maximum a posterior) and obtained an adaptive regularizer learning method ($i.e.$ low rank approximation regularized by Logarithm on singular values). In this paper, we extend the method and use the l_1 norm of the logistic function on the singular values of a matrix to replace the nuclear norm as the low-rank constraint. In summary, the main contributions of this paper are as follows:

- Our low rank regularization is motivated by the Bayesian perspective. It is based on a hypothesis that the singular values of a matrix fit Laplacian distribution with varying scale parameters [15]. Compare to the traditional nuclear norm minimization model, our model achieved better performance. Furthermore, we solve the optimization problem by the alternating direction method (ADM) and the Logarithm regularizer used in model has closed form solution.
- Rather than the tree-structured sparsity-inducing norm in [3] based on a tree structure, we just adopt a weighed group sparsity norm regularization to explore the relationship between each superpixel. Because the index tree is a hierarchical structure, the segmentation process of the input image is more complex. In order to improve the efficiency of segmentation, we proposed the group sparsity induced norm. It not only has less operation time, but also can achieve the same effect.

II. Related Work

In this section, we briefly review the related work on salient object detection. Because both the bottom-up and top-down models have a certain degree of limitation. Recent research has focused on combination of both. In recent years, the low-rank matrix recovery (LRMR) model [17]

*Corresponding author

0-7695-6341-4/17/31.00 ©2017 IEEE
DOI 10.1109/CIS.2017.00034

has motivated many kinds of models. For example, Shen et al. proposed a unified low-rank model (ULR) by learning linear transformation of the feature space to integrate low-level features and high-level priors knowledge. In [18], Lang et al. suggested a multi-task sparsity pursuit model (MSP) to combinate multiple types of features collaboratively in salient object detection. In [19], Zou et al. applied a segmentation driven low-rank matrix recovery model (SLR), where the matrix recovery model was guided by a bottom-up segmentation prior. Peng et al. [2] [3] presented a low-rank and tree-structured sparse matrix decomposition model (SMD) to seek the underlying structure of image patches. However, all of those methods deal with the low-rank part by using the nuclear norm to approximate the low-rank constraint, which may be a loose approximation and lead to over-penalized problem. In [15], Jia et al. proposed an adaptive regularizer learning method in the framework of MAP (maximum a posterior). Inspired by this, we present a novel low-rank regularization that regularized by Logarithm on singular values and have achieved better performance.

III. Nonconvex Structured Matrix Decomposition Model

A. Basic Formulation

In order to get homogeneous consistent regions, we use SLIC [4] to over-segment the image into N non-overlapping patches $\{B_i\}_{i=1,...,N}$, where N is the number of segmentations. For each B_i, a D dimensional feature vector is extracted and denoted as f_i. Then these feature vectors form a feature matrix $F = [f_1, f_2, ..., f_N] \in R^{D\times N}$. Then, we consider an image as a combination of low-rank matrix and sparse matrix. Therefore, F can be decomposed into two parts $F = L + S$. Our model can be formulated as:

$$\begin{aligned} &\min_{L,S} \Phi(L) + \alpha\Upsilon(S) + \beta\Theta(L, S) \\ &s.t.\ F = L + S \end{aligned} \tag{1}$$

where $\Phi(L) = \sum_{i=1}^{r} \log(\sigma_i + \varepsilon)$ is the non-convex low rank regularization. $\Upsilon(S) = \sum_{i=1}^{n} \omega_i \|S_{G_i}\|_F$ is the weighed group sparsity norm regularization. $\Theta(L, S) = Tr(SH_F S^T)$ is Laplacian regularization. And α, β are positive tradeoff parameters. Accordingly, the Eq.(1) can be rewritten as:

$$\begin{aligned} &\min_{L,S} \sum_{i=1}^{r} \log(\sigma_i + \varepsilon) + \alpha \sum_{i=1}^{n} \omega_i \|S_{G_i}\|_F + \beta Tr(SH_F S^T) \\ &s.t.\ F = L + S \end{aligned} \tag{2}$$

B. Non-convex Low Rank Regularization

Motivated by the theory in [12], the reference [15] obtained an adaptive regularizer learning method by seeking an appropriate scale parameter. Inspired by this, we propose our nonconvex low-rank regularization in the salient object detection. Therefore, low rank matrix recovery problem in our model can be formulated as:

$$\min_{\Sigma} \sum_{i=1}^{r} \log(\sigma_i + \varepsilon) \tag{3}$$

where r is the rank and σ_i is the i-th singular value of L. In order to guarantee the stability of the algorithm, we introduce an arbitrary small positive constant ε. In addition, the work of [15] proved that Logarithm regularizer used in model has closed form solution.

C. Group Sparsity Norm Regularization

A valid segmentation result usually contains some useful information of the image. So, we can impose it on the salient part S as a constraint, which is encoded by a group sparsity norm in our model, defined as follows:

$$\Upsilon(S) = \sum_{i=1}^{n} \omega_i \|S_{G_i}\|_F \tag{4}$$

where $\omega_i > 0$ is a weight corresponding to the node G_i as the prior, and S_{G_i} is a sub-matrix of S corresponding to i-th node G_i in the graph. $S_{G_i} \in R^{D\times|G_i|}$ ($\|\cdot\|$ is the cardinality of a set), n is the number of nodes. Actually, $\Upsilon(S)$ is the weighted group sparsity norm [13]. In addition, our group sparsity norm $\Upsilon(S)$ forces the patches within the same group to share more similar representations while the patches from different groups to have different representations.

D. Laplacian Regularization

As all known, it is difficult for traditional matrix decomposition models to separate the salient region from the background when the two parts are extremely similar or the background is complicated. Therefore, when decomposing the feature matrix F into a low-rank part L plus a structured-sparse part S, we hope to increase the margin between the subspaces induced by L and S. To this end, we introduce a Laplacian regularization as [3]. We define the regularization as:

$$\Theta(L, S) = \frac{1}{2} \sum_{i,j=1}^{N} \upsilon_{i,j} \|s_i - s_j\|_2^2 = Tr(SH_F S^T) \tag{5}$$

where s_i is the i-th column of sparse matrix S, and $\upsilon_{i,j}$ denotes the similarity of patches (B_i, B_j). It is defined as:

$$\upsilon_{i,j} = \begin{cases} e^{(-\frac{\|f_i - f_j\|^2}{2\sigma^2})}, & B_i \in \mathcal{N}(B_j)\ or\ B_j \in \mathcal{N}(B_i) \\ 0, & otherwise \end{cases} \tag{6}$$

where $\mathcal{N}(B_i)$ denotes the set of neighbors of B_i. It forms a symmetric weight matrix $V \in R^{N\times N}$. And $H_F = D - V$ is the graph Laplacian matrix corresponding to the weight matrix V and its degree matrix D. The degree matrix D is a diagonal matrix and its i-th entry D_{ii} corresponds to the summation of all the similarities related to B_i, $i.e.$, $D_{ii} = \sum_j \upsilon_{ij}$, which is also mentioned in [14].

E. High-level Priors Integration

Motivated by Shen and Wu [1], we get a prior map by integrating the gaussian distribution of color, location and background priors [16] into our model. Then high-level priors are also embedded into our model as the weights. The prior value π_i for each superpixel represents the possibility, $i.e.$, whether superpixel B_i is the salient object or not. In particular, we define ω_i as:

$$\omega_i = 1 - \max(\{\pi_i : B_i \in G_i\}) \tag{7}$$

This means that the nodes with small prior values are imposed a large punishment, and vice versa. The complete algorithm is presented in **Algorithm**1. And we will explain the details in the next section.

Algorithm 1 The proposed algorithm

Input: Feature matrix F, parameters α,β, group $G = \{G_i\}_1^n$ and the prior weight ω_i.
Step 1: Initialize $L^0 = 0$, $S^0 = 0$, $J^0 = 0$, ${Y_1}^0 = 0$, ${Y_2}^0 = 0$, $\mu = 0.1$, $\mu_{max} = 10^6$, $\rho = 1.1$, $k = 0$.
Step 2: **While** not converged **do**
Step 3: $L^{k+1} = \arg\min\limits_{L} \mathcal{L}(L, S^k, J^k, {Y_1}^k, {Y_2}^k, \mu^k)$
Step 4: $J^{k+1} = \arg\min\limits_{J} \mathcal{L}(L^k, S^k, J, {Y_1}^k, {Y_2}^k, \mu^k)$
Step 5: $S^{k+1} = \arg\min\limits_{S} \mathcal{L}(L^k, S, J^k, {Y_1}^k, {Y_2}^k, \mu^k)$
Step 6: ${Y_1}^{k+1} = {Y_1}^k + \mu^k(F - L^{k+1} - S^{k+1})$
Step 7: ${Y_2}^{k+1} = {Y_2}^k + \mu^k(S^{k+1} - J^{k+1})$
Step 8: $\mu^{k+1} = \min(\rho\mu^k, \mu_{max})$
Step 9: $k = k + 1$
Step 10: **End While**
Output: L^k and S^k

IV. Optimization Method for Solving Our Model

In this paper, the alternating direction method (ADM) is applied to solve our proposed optimization problem. Firstly we introduce an auxiliary variables J, corresponding to S in Eq.(2). The augmented Lagrangian function of Eq.(2) is:

$$\begin{array}{l} \min\limits_{L,S} \sum\limits_{i=1}^{r} \log(\sigma_i + \varepsilon) + \alpha \sum\limits_{i=1}^{n} \omega_i \|S_{G_i}\|_F + \beta Tr(JH_F J^T) \\ s.t.\ F = L + S,\ S = J \end{array} \tag{8}$$

In order to transform the constrained optimization problem Eq.(8) to an unconstrained optimization problem, we introduce two Lagrange multipliers Y_1 and Y_2. Then, Eq.(8) is equivalent to the following problem:

$$\begin{array}{l} \mathcal{L}(L, S, J, Y_1, Y_2, \mu) = \sum\limits_{i=1}^{r} \log(\sigma_i + \varepsilon) + \alpha \sum\limits_{i=1}^{n} \omega_i \|S_{G_i}\|_F \\ + \beta Tr(JH_F J^T) + Tr({Y_1}^T(F - L - S)) \\ + Tr({Y_2}^T(S - J)) + \frac{\mu}{2}(\|F - L - S\|_F^2 + \|S - J\|_F^2) \end{array} \tag{9}$$

where μ is a penalty parameter, and $\|\cdot\|_F^2$ is the matrix Frobenius norm defined as $\|X\|_F^2 = \sum\limits_{i=1}^{m}\sum\limits_{j=1}^{n} |x_{ij}|^2$. This problem can be optimized by alternately updating one variable while others fixed. In the following, we describe each iteration respectively.

A. Computation of L

Fixing S and J, to seek L, we get the following optimization problem,

$$\begin{array}{l} \mathcal{L}_1 = \arg\min\limits_{L} \sum\limits_{i=1}^{r} \log(\sigma_i + \varepsilon) + Tr({Y_1}^T(F - L - S)) \\ \qquad + \frac{\mu}{2}\|F - L - S\|_F^2 \\ \quad = \arg\min\limits_{L} \sum\limits_{i=1}^{r} \log(\sigma_i + \varepsilon) + \frac{1}{2\tau}\|L - M_L\|_F^2 \end{array} \tag{10}$$

where $\tau = \frac{1}{\mu}$ and $M_L = F - S + \frac{Y_1}{\mu}$. The solution to Eq.(10) has briefly mentioned in the above section. Firstly, we obtain the singular values of matrix M_L based on singular value decomposition (SVD): $(U, \Sigma_{M_L}, V^T) = \mathcal{SVD}(M_L)$, where $\Sigma_{M_L} = \operatorname{diag}(\sigma_{M_i})_{i=1,\ldots,r}$, The Eq.(10) is equivalent to solve:

$$\arg\min_{\sigma_i} \log(\sigma_i + \varepsilon) + \frac{1}{2\tau}(\sigma_{M_i} - \sigma_i)^2 \tag{11}$$

The Euler-Lagrange equation of the energy in Eq.(11) is:

$$\sigma_i - \sigma_{M_i} + \frac{\tau}{\sigma_i + \varepsilon} = 0 \tag{12}$$

It has closed form solution [15]:

$$\sigma_i = \begin{cases} \frac{(\sigma_{M_i} - \varepsilon) + \sqrt{(\sigma_{M_i} - \varepsilon)^2 - 4(\tau - \sigma_{M_i}\varepsilon)}}{2}, & i \in I_1 \\ 0 & , i \in I_2 \end{cases} \tag{13}$$

$I_1 = \left\{ i \left| (\sigma_{M_i} - \varepsilon)^2 - 4(\tau - \sigma_{M_i}\varepsilon) \geq 0 \right.\right\}$, and $I_2 = \left\{ i \left| (\sigma_{M_i} - \varepsilon)^2 - 4(\tau - \sigma_{M_i}\varepsilon) < 0 \right.\right\}$, where σ_{M_i} is the i-th singular value of M_L. Then we get the i-th singular value σ_i of L. Finally, we obtain $L = U\Sigma V^T$.

B. Computation of J

When S and L are fixed, updating J is equivalent to optimize the following function,

$$\begin{array}{l} \mathcal{L}_2 = \arg\min\limits_{J} \beta Tr(JH_F J^T) + Tr({Y_2}^T(S - J)) \\ \qquad + \frac{\mu}{2}\|S - J\|_F^2 \end{array} \tag{14}$$

The Euler-Lagrange equation of energy in Eq.(14) is:

$$\beta(JH_F + J{H_F}^T) - {Y_2}^T - \mu(S - J) = 0 \tag{15}$$

Because H_F is symmetrical, we have $J(2\beta H_F + \mu I) = {Y_2}^T + \mu S$. Then we get:

$$J = ({Y_2}^T + \mu S)(2\beta H_F + \mu I)^{-1} \tag{16}$$

C. Computation of S

We update S while L and J are fixed. Then we get the optimization problem as follows,

$$\begin{aligned}\mathcal{L}_3 &= \arg\min_S \alpha \sum_{i=1}^{n} \omega_i \|S_{G_i}\|_F + Tr({Y_1}^T(F-L-S)) \\ &+Tr({Y_2}^T(S-J)) + \tfrac{\mu}{2}(\|F-L-S\|_F^2 + \|S-J\|_F^2) \\ &= \arg\min_S \lambda \sum_{i=1}^{n} \omega_i \|S_{G_i}\|_F + \tfrac{1}{2}\|S-M_S\|_F^2\end{aligned} \tag{17}$$

where $M_S = \frac{1}{2}(F-L+J+(\frac{Y_1-Y_2}{\mu}))$, and $\lambda{=}\frac{\alpha}{2\mu}$. This optimization problem can be solved by the proximal operator, which is equal to compute the orthogonal projection of the matrix onto the ball of the dual norm $\|\cdot\|_F^2$. Details are described in **Algorithm**2.

Algorithm 2 Solving the group sparsity

Input: The segmentation graph G with the set of nodes G_i, weight ω_i, the matrix M_S, parameter $\alpha = 1.1$, and we set $\lambda{=}\frac{\alpha}{2\mu}$.

Step 1: Initialize $S = M_S$

Step 2: **for** $i = 1 \rightarrow n$ **do**

Step 3: $S_{G_i}^{k+1} = \begin{cases} \frac{\|S_{G_i}\|_F - \lambda\omega_i}{\|S_{G_i}\|_F} S_{G_i}, & if \|S_{G_i}\|_F > \lambda\omega_i \\ 0, & otherwise \end{cases}$

Step 4: $i = i + 1$

Step 5: **end for**

Output: S

V. Experiments

A. Parameter Setting

In this section, we evaluate our model on the ECSSD dataset. We set the segmentation threshold is $T = 2000$ to obtain a graph. The bandwidth parameter in our model is set to be $\delta = 0.05$. And the tradeoff parameters are set to be $\alpha = 1.1$, $\beta = 0.35$ respectively.

B. Evaluation Metrics

For evaluation, we use two metrics, including PR curve and mean absolute error (MAE). Precision refers to the fraction of salient pixels correctly assigned in the result of saliency detection, while recall corresponds to the fraction of samples categorized as positive that are correctly labels. In addition, MAE measures the dissimilarity between the saliency map and the ground truth. It is the average per-pixel difference between ground truth and binary saliency map, normalized to $[0, 1]$, which is defined as:

$$MAE = \frac{1}{W \times H} \sum_{x=1}^{W} \sum_{y=1}^{H} |S(x,y) - GT(\mathrm{x},y)| \tag{18}$$

where W and H are the width and height of the respective saliency map S, and GT is the ground truth saliency map.

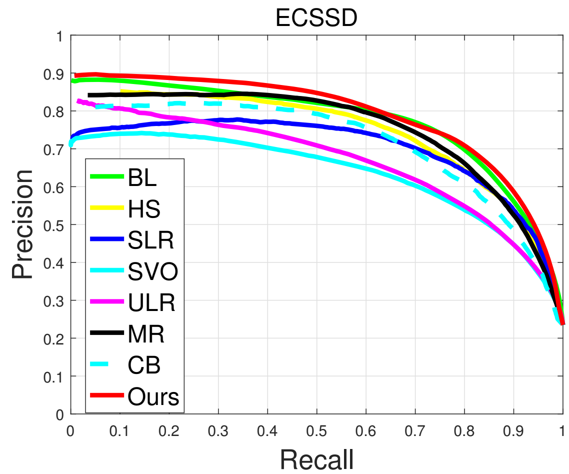

Figure 1. PR Curves of different methods on the ECSSD dataset, and the result shows that our method has better performance.

Table I
Results on the ECSSD dataset in term of MAE.

Metric	OUR	MR	BL	SLR	HS	CB	ULR	SVO
MAE	**0.178**	0.186	0.216	0.226	0.227	0.240	0.274	0.412

C. Results on ECSSD

Our model is evaluated on the widely used ECSSD dataset and compared with seven state-of-the art methods, including BL [20], MR [22], SLR [19], HS [21], CB [23], ULR [1], SVO [24]. Fig.1 represents the PR curves using the previous models and our proposed model. The result shows that the PR curves of our method is higher than other methods. For further understanding of our model, we also display the comparison results of MAE in Table I and our proposed method get the better results. Finally, some examples of different methods are shown in Fig.2.

VI. Conclusion

In this paper, a nonconvex structured matrix decomposition model is presented. In our model, we adopt the l_1 norm of the logistic function on the singular values of a matrix to replace the nuclear norm. In addition, we introduce a weighed group sparsity norm regularization to explore the relationship between each superpixel. We also add the Laplacian regularization to reduce the coherence between the low-rank and group sparse matrices. At last, high-level priors are integrated into the model to boom the performance. Experiments on the widely used ECSSD dataset show that the proposed model outperforms the state-of-the-art models.

Acknowledgment

This work is supported by the National Natural Science Funds of China (Grant Nos. 61472257).

(a) Image (b) SVO (c) ULR (d) CB (e) HS (f) SLR (g) BL (h) MR (i) Ours (j) GT

Figure 2. The examples of saliency detection by the proposed method and other seven methods have shown that our method achieve the best performance and the salient maps are very close to the ground truth(GT).

REFERENCES

[1] X.-H. Shen, Y. Wu, *A unified approach to salient object detection via low rank matrix recovery*, in CVPR. IEEE, 2012, pp. 2296-2303.

[2] H. Peng, B. Li, R. Ji, W. Hu, W. Xiong, *Salient object detection via low-rank and structured sparse matrix decomposition*, in AAAI, 2013, pp. 796-802.

[3] H. Peng, H. Ling, W. Hu, *Salient object detection via structured matrix decomposition*, IEEE Trans. Pattern Anal. Mach. Intell. 99 (2016) 1-14.

[4] R. Achanta, A. Shaji, K. Smith, A. Lucchi, P. Fua, and S. Süsstrunk, *Slic superpixels compared to state-of-the-art superpixel methods*, IEEE Trans. Pattern Anal. Mach. Intell. 34(11) (2012) 2274-2282.

[5] L. Itti, C. Koch, E. Niebur, *A model of saliency-based visual attention for rapid scene analysis*, IEEE Trans. Pattern Anal. Mach. Intell. 20(11) (1998) 1254-1259.

[6] J. Han, D. Zhang, S. Wen, L. Guo, T. Liu, X. Li, *Two-stage learning to predict human eye fixations via SDAEs*, IEEE Trans. Syst. Man Cybern. 46(2) (2016) 487-498.

[7] M. Donoser, M. Urschler, M. Hirzer, and H. Bischof, *Saliency driven total variation segmentation*, in ICCV. IEEE, 2009, pp. 817-824.

[8] C. Guo and L. Zhang, *A novel multiresolution spatiotemporal saliency detection model and its applications in image and video compression*, IEEE transactions on image processing. 19(1) (2010) 185-198.

[9] S. Frintrop, G. M. Garcia, and A. B. Cremers, *A cognitive approach for object discovery*, in ICPR. IEEE, 2014, pp. 2329-2334.

[10] M.-M. Cheng, G.-X. Zhang, N. J. Mitra, X. Huang, and S.-M. Hu, *Global contrast based salient region detection*, in CVPR. IEEE, 2011, pp. 409-416.

[11] Q. Wang, W. Zheng, and R. Piramuthu, *GraB: Visual saliency via novel graph model and background priors*, in CVPR. IEEE, 2016, pp. 535-543.

[12] C. Lu, J. Tang, S. Yan, et al. *Generalized nonconvex nonsmooth low-rank minimization*, in CVPR. IEEE, 2014, pp. 4130-4137.

[13] X.-L. Sun, Z.-X. He, C. Xu, et al. *Diversity induced matrix decomposition model for salient object detection*, Pattern Recognition. 66 (2017) 253-267.

[14] M. Yin, J. Gao, Z. Lin, *Laplacian regularized low-rank representation and its applications*. IEEE Trans. Pattern Anal. Mach. Intell. 38(3) (2016) 504-517.

[15] X.-X. Jia, X.-C Feng, W.-W Wang, *Adaptive regularizer learning for low rank approximation with application to image denoising*, in ICIP. IEEE, 2016, pp. 3096-3100.

[16] W.-J. Zhu, S. Liang, Y.-C. Wei, and J. Sun, *Saliency optimization from robust background detection*, in CVPR. IEEE, 2014, pp. 2814-2821.

[17] E. Candès, X. Li, Y. Ma, and J. Wright, *Robust principal compnent analysis*, JACM, 58(3) (2011) 1-39.

[18] C.-Y. Lang, G.-C. Liu, J. Yu, and S.-C. Yan, *Saliency detection by multitask sparsity pursuit*, IEEE transactions on image processing. 21(3) (2012) 1327-1338.

[19] W.-B. Zou, K. Kpalma, Z. Liu, and J. Ronsin, *Segmentation driven low-rank matrix recovery for saliency detection*, in BMVC, 2013, pp. 1-13.

[20] N. Tong, H. Lu, X. Ruan, M.-H. Yang, *Salient object detection via bootstrap learning*, in CVPR. IEEE, 2015, pp. 1884-1892.

[21] Q. Yan, L. Xu, J. Shi, J. Jia, *Hierarchical saliency detection*, in CVPR, IEEE, 2013, pp. 1155-1162.

[22] C. Yang, L. Zhang, H. Lu, X. Ruan, M.-H. Yang, *Saliency detection via graph-based manifold ranking*, in CVPR. IEEE, 2013, pp. 3166-3173.

[23] H. Jiang, J. Wang, Z. Yuan, *Automat salient object segmentation based on context and shape prior*, in BMVC, 2011, pp. 1-12.

[24] K.-Y. Chang, T.-L. Liu, H.-T. Chen, S.-H. Lai, *Fusing generic objectness and visual saliency for salient object detection*, in ICCV. IEEE, 2011, pp. 914-921.